

# Comparison of a Pair of Synthetic Tea-Catechin-Derived Epimers: Synthesis, Antifolate Activity, and Tyrosinase-Mediated Activation in Melanoma

Magalí Sáez-Ayala,<sup>[a]</sup> Luis Sánchez-del-Campo,<sup>[a]</sup> María F. Montenegro,<sup>[a]</sup> Soledad Chazarra,<sup>[a]</sup> Alberto Tárraga,<sup>[b]</sup> Juan Cabezas-Herrera,<sup>[c]</sup> and José Neptuno Rodríguez-López\*<sup>[a]</sup>

Despite bioavailability issues, tea catechins have emerged as promising chemopreventive agents because of their efficacy in various animal models. We synthesized two catechin-derived compounds, 3-*O*-(3,4,5-trimethoxybenzoyl)-(-)-catechin (TMCG) and 3-*O*-(3,4,5-trimethoxybenzoyl)-(-)-epicatechin (TMECG), in an attempt to improve the stability and cellular absorption of tea polyphenols. The antiproliferative and pro-apoptotic activi-

ties of both compounds were analyzed with various cancer cell systems, and TMCG, which was easily synthesized in excellent yield, was more active than TMECG in both melanoma and non-melanoma cell lines. TMCG was also a better inhibitor of dihydrofolate reductase and was more efficiently oxidized by tyrosinase, potentially explaining the difference in activity between these epimers.

## Introduction

We have recently shown that the ester-bonded gallate catechins isolated from green tea, epigallocatechin-3-gallate (EGCG) and epicatechin-3-gallate (ECG), are potent inhibitors of dihydrofolate reductase (DHFR) activity *in vitro* at concentrations found in the serum and tissues of green tea drinkers.<sup>[1]</sup> Since this first report describing the antifolate activity of tea polyphenols, several studies by us and other research groups have confirmed this activity<sup>[2–4]</sup> and reported that EGCG inhibits DHFR from a variety of biological sources.<sup>[5–8]</sup> Recently, screening of DHFR binding drugs by MALDI-TOF MS demonstrated that EGCG is an inhibitor of DHFR with a relative affinity between that of pyrimethamine and methotrexate (MTX).<sup>[8]</sup> However, the excellent anticancer properties of tea catechins are significantly limited by their poor bioavailability, which is related to their low stability in neutral or slightly alkaline solutions and their inability to easily cross cellular membranes.<sup>[9]</sup> In an attempt to solve these bioavailability problems, we synthesized a 3,4,5-trimethoxybenzoyl analogue of ECG (TMECG, **6**; Scheme 1) that exhibits high antiproliferative activity against malignant melanoma but considerably lower activity against other epithelial cancer cell lines.<sup>[10]</sup> This compound acts as a prodrug against melanoma and is selectively activated by the specific melanocyte enzyme tyrosinase.<sup>[11]</sup> Upon activation, TMECG generates a stable quinone methide that strongly and irreversibly inhibits DHFR. TMECG treatment induces apoptosis in melanoma cells and results in the downregulation of anti-apoptotic Bcl-2, the upregulation of pro-apoptotic Bax, and the activation of caspase-3.<sup>[12]</sup>

Because the major polyphenols present in tea have epicatechin configurations, many of the studies designed to elucidate the biological activity of these tea catechins have been performed with epicatechin derivatives. However, (-)-catechin gallate (CG), which is a minor polyphenol in green tea, also inhibits the proliferation of cancer cells derived from human oral

cavity tissues.<sup>[13]</sup> As part of our ongoing efforts to develop new tea-derived compounds, we synthesized a trimethoxybenzoyl analogue of CG (TMCG, **8**; Scheme 1). This compound shares bioavailability advantages with its epimer, TMECG, due to their similar hydrophobicities, and is simpler and more economical to synthesize. This enabled us to compare the epimeric differences between TMECG and TMCG with respect to DHFR inhibition, tyrosinase activation, and antiproliferative action against various cancer cell systems.

## Results and Discussion

### Comparative synthesis of TMECG and TMCG

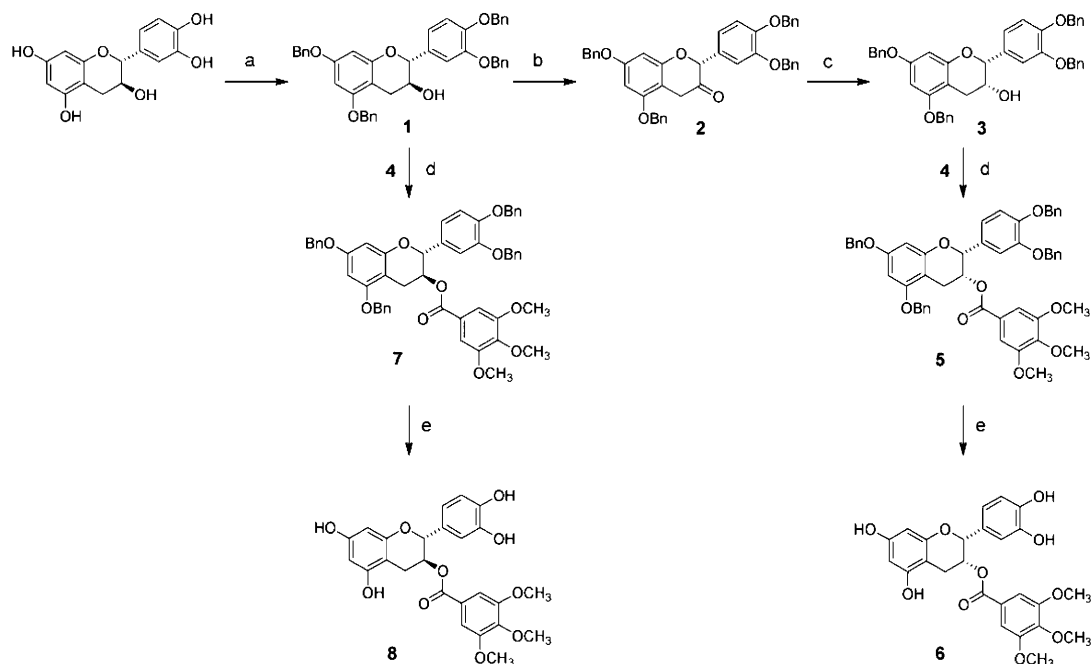
Synthesis of TMECG, starting from the commercially available catechin, was previously described by our research group.<sup>[10]</sup> The reaction sequence was designed to avoid problems associated with unspecific blockage of the 3-hydroxy group of epica-

[a] M. Sáez-Ayala, Dr. L. Sánchez-del-Campo, Dr. M. F. Montenegro, Dr. S. Chazarra, Dr. J. N. Rodríguez-López  
Department of Biochemistry and Molecular Biology A  
School of Biology, University of Murcia  
Avda. Teniente Flomesta, no. 5, 30003 Murcia (Spain)  
Fax: (+34) 868-884147  
E-mail: neptuno@um.es

[b] Prof. A. Tárraga  
Department of Organic Chemistry  
Faculty of Chemistry, University of Murcia  
Avda. Teniente Flomesta, no. 5, 30003 Murcia (Spain)

[c] Dr. J. Cabezas-Herrera  
Research Unit of Clinical Analysis Service  
University Hospital "Virgen de la Arrixaca"  
Ctra. Madrid-Cartagena, 30120 Murcia (Spain)

Supporting information for this article is available on the WWW under <http://dx.doi.org/10.1002/cmdc.201000482>.



**Scheme 1.** Synthesis of TMECG (**6**) and TMCG (**8**): a) BnBr,  $K_2CO_3$ , DMF,  $-10\text{ }^\circ\text{C}$ —RT, overnight; b) Dess–Martin periodinane,  $CH_2Cl_2$ , RT, 3 h; c) L-Selectride,  $nBu_4NCl$ , THF,  $-78\text{ }^\circ\text{C}$ , 3 h; d) 3,4,5-trimethoxybenzoyl chloride, **4**,  $CH_2Cl_2$ , DMAP, RT, 18 h; e)  $H_2$ , 20% Pd/C, THF/MeOH (3:1), RT, 14 h.

techin following the benzylation reaction with benzyl bromide and potassium carbonate.<sup>[14,15]</sup> Therefore, all compounds (both catechin and epicatechin configurations) were synthesized following the multi-step reaction sequence shown in Scheme 1. For the synthesis of TMCG (**8**), isomer **1** was esterified with previously prepared<sup>[10]</sup> 3,4,5-trimethoxybenzoyl chloride **4** in a dichloromethane solution in the presence of DMAP, producing **7** in high yield. In the final step, the benzyl groups were removed by hydrogenolysis to produce final compound **8** in high yield and purity. TMECG and TMCG have a common first synthetic step, but yields of the other synthetic steps are significantly different. The overall yield of **8** for the alkylation and deprotection steps was 88%; however, an overall yield of 16% was obtained for **6** in the epimerization of C3 (oxidation and reduction), alkylation, and deprotection steps. The difference between these yields was due to the stereoselective reduction of **2**, which results in only moderate yield and purity and requires further purifications, thereby lowering the yield. The absence of this limiting step makes the synthesis of **8** both simpler (only three steps) and more economical (only common reagents).

#### Activity in non-melanoma cells

In studying the antiproliferative activity of TMECG, we noted that this compound was more active against melanoma than against other epithelial cancer cell lines.<sup>[10,11]</sup> TMECG inhibited the growth of human breast (MDA-MB-231), lung (N417), and colon (Caco-2) cancer lines with half-maximal inhibitory concentrations ( $IC_{50}$ ) at six days of  $21 \pm 1.5$ ,  $18 \pm 2.1$ , and  $33 \pm 3.1\ \mu\text{M}$ , respectively (Figure 1A). The high concentrations of TMECG required to inhibit the growth of these cells suggest

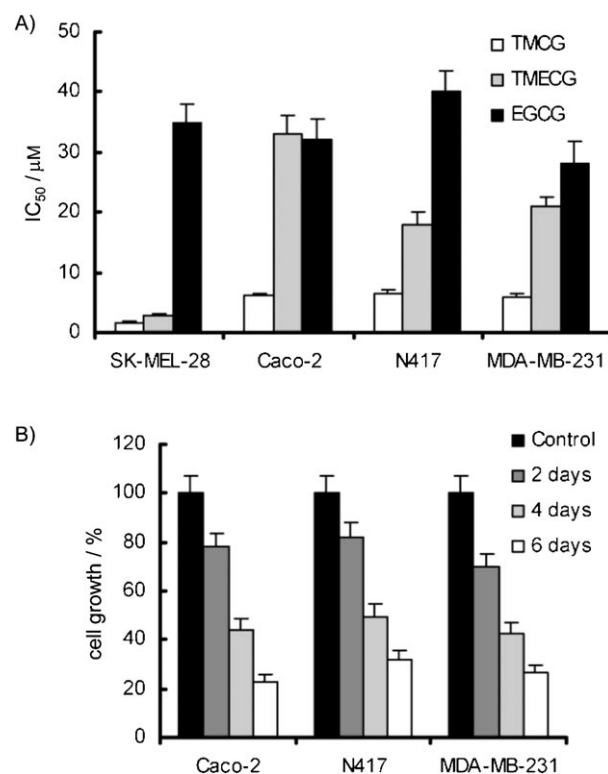


**Figure 1.** Antiproliferative effects of natural and synthetic catechins in cancer cells. A) Half-maximal inhibitory concentration ( $IC_{50}$ ) of TMCG and TMECG against several melanoma and non-melanoma cells after six days of treatment. Differences between the effects of TMCG and TMECG were statistically significant in all treated cells ( $p < 0.05$ ). EGCG data are included for comparison. B) Time-dependent effect of TMCG ( $10\ \mu\text{M}$ ) on the growth of non-melanoma cancer cells. At each time point, the percentage of cell growth was calculated with respect to the growth of an untreated control (100%).

that this compound would not be therapeutically useful. However, TMCG was much more active against these cancer cell lines and significantly inhibited cell growth with  $IC_{50}$  values at six days of  $5.9 \pm 0.5$ ,  $6.6 \pm 0.6$ , and  $6.2 \pm 0.4 \mu\text{M}$  against MDA-MB-231, N417, and Caco-2, respectively (Figure 1A). The time-dependent effect of TMCG on non-melanoma cancer cell growth can be visualized in Figure 1B. In addition to inhibiting cell proliferation, chemotherapeutic agents should ideally induce apoptosis; therefore, TMCG was analyzed to determine its ability to induce apoptosis. TMCG induced apoptosis in these epithelial cancer cell lines at a relatively low concentration, as demonstrated by the significant morphological changes induced by treatment including cell shrinkage, loss of cell–cell contact, and fragmentation of plasmatic and nuclear membranes (Figure 2A). To confirm the apoptotic activity of TMCG, Annexin-V and propidium iodide were used to examine early and late stages of apoptosis, respectively. Conjugated Annexin-V–fluorescein was used to determine the translocation of phosphatidylserine from the inner part of the plasma membrane to the outer layer, which is an early feature of apoptosis; propidium iodide was used to stain the DNA of cells in very late stages of apoptosis. Figure 2B shows histograms of MDA-MB-231 cells stained with Annexin-V–fluorescein and propidium iodide as obtained by flow cytometry. We detected a concentration-dependent increase in the total number of apoptotic cells reaching  $\sim 40\%$  upon treatment with  $40 \mu\text{M}$  TMCG for 96 h. Together, these data indicate that TMCG could be an effective anticancer agent with growth inhibitory and apoptotic effects.

#### Mechanistic studies to explain the differential action of TMCG and TMECG against non-melanoma cells

Although many epidemiological and laboratory studies support the beneficial health effects of green tea consumption, the exact mechanism of action of its polyphenolic compounds is subject to continuous debate. Most plant polyphenols possess both antioxidant and pro-oxidant properties, and it has

frequently been suggested that the pro-oxidant action of polyphenols may be important to their anticancer and apoptosis-inducing properties.<sup>[16]</sup> TMECG and TMCG possess similar antioxidant and pro-oxidant properties (Table 1), indicating that

**Table 1.** Mechanistic studies to explain the differential action of TMCG and TMECG in non-melanoma cells.

Possible mechanism	EGCG <sup>[a]</sup>	TMECG	TMCG
<i>Antioxidant</i>			
TEAC <sup>[b]</sup> [mM]	$4.8 \pm 0.3$	$1.9 \pm 0.2$	$2.0 \pm 0.2$
<i>Pro-oxidant</i>			
NADPH consumption [nM min <sup>-1</sup> ]	$149 \pm 8$	$11.4 \pm 2$	$12.1 \pm 3$
<i>Inhibition of proteasome</i>			
$IC_{50}$ [ $\mu\text{M}$ ]	$0.2 \pm 0.1$ <sup>[c]</sup>	> 40	> 40
<i>Inhibition of DHFR</i>			
$K_i$ [ $\mu\text{M}$ ]	$1.2 \pm 0.1$	$2.1 \pm 0.2$	$0.9 \pm 0.1$
$K_i^*$ [nM]	$33 \pm 3$	$110 \pm 9$	$18 \pm 2$

[a] EGCG data are included for comparison. [b] TEAC=trolox equivalent antioxidant capacity. [c] Data taken from reference [20].

these properties are not responsible for the differential biological effects of these two compounds in non-melanoma epithelial cancer cells. A number of additional mechanisms, including the impact of EGCG on a wide range of molecular targets that influence cell growth and apoptosis, have been proposed as causes for the anticancer effects of this polyphenolic compound.<sup>[1,17–19]</sup> The 3-gallyl moiety of catechins is essential to the modulation of several molecular targets.<sup>[1,17–19]</sup> Because EGCG inhibits the chymotrypsin-like activity of the proteasome (Table 1), inhibition of this multicatalytic protease was proposed as a general mechanism for the biological effects of tea catechins.<sup>[18–20]</sup> However, methylation of the 3-gallyl moiety suppresses the proteasome-inhibitory function of green tea polyphenols.<sup>[20]</sup> Correspondingly, TMECG and TMCG do not significantly inhibit the chymotrypsin-like activity of purified rabbit 20S proteasome (Table 1). Although inhibition of the

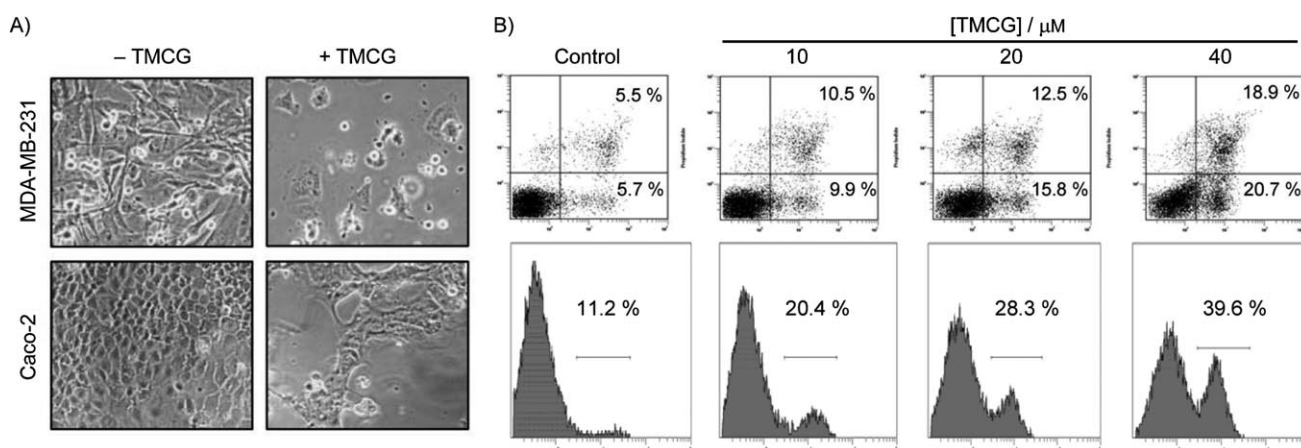


**Figure 2.** Induction of apoptosis by TMCG in cancer cells. A) Morphological aspect of untreated MDA-MB-231 and Caco-2 cells compared with those subjected to five days of treatment with  $20 \mu\text{M}$  TMCG. B) Histograms of MDA-MB-231 cells stained with Annexin-V–fluorescein and propidium iodide (PI) with and without TMCG treatment. Dot plots show percentages of early apoptotic cells (Annexin-V<sup>+</sup>/PI<sup>-</sup>) and late apoptotic cells (Annexin-V<sup>+</sup>/PI<sup>+</sup>). Histograms show gates indicating percentages of total apoptotic cells.

proteasome by EGCG may be biologically significant in several isolated cell systems, as a general mechanism of action for tea polyphenols it does not account for much of the epidemiological data, as liver methylation of catechins is one of the major biotransformation reactions under physiological conditions.<sup>[21]</sup> Therefore, metabolic methylation of catechin, leading to methylated EGCG, may alter the biological activities of this compound.<sup>[22]</sup>

In contrast, epimeric differences, which could explain the biological data, were observed with respect to the inhibition of DHFR, another potential target of green tea polyphenols.<sup>[1,6]</sup> Kinetic analyses indicated that TMECG was a more efficient inhibitor of this enzyme than TMECG. Analysis of the binding of these polyphenols to human DHFR using fluorescence quenching indicated that TMECG bound to the enzyme with a lower dissociation constant ( $K_i$ ) than TMECG (Table 1). Pre-incubation of human DHFR with TMECG or TMECG confirmed that both compounds had the characteristics of slow-binding inhibitors of human DHFR (Figure 3A),<sup>[1,5,6]</sup> but pre-incubation of the enzyme with TMECG had a more profound effect on enzymatic activity. Complete kinetic analysis, assuming isomerization to a slowly dissociating inhibition complex ( $E + I \rightleftharpoons EI \rightleftharpoons E^*I$ ),<sup>[5]</sup> demonstrated that the overall inhibition constant ( $K_i^*$ ), which is affected by further EI-complex reactions, decreased dramatically when TMECG acted as an inhibitor of human DHFR (Table 1). Together, the results indicate that the  $EI \rightleftharpoons E^*I$  transition was irreversible to a greater extent with TMECG, which possesses a catechin configuration.

### Molecular modeling

In silico molecular modeling experiments performed in our laboratory indicated that TMECG bound to human DHFR in a fashion similar to the binding of EGCG, another natural tea phenol with an epicatechin configuration.<sup>[1,11]</sup> The most notable interaction between TMECG and DHFR was a hydrogen bond between the ring A hydroxy group of TMECG and Glu30 in the enzyme active site (O–O distance 2.94 Å) (Figure 3B). Comparison of a range of DHFR structures containing folate or other inhibitors shows that a majority of the TMECG lies within the consensual substrate/inhibitor envelope, with the exception of the non-ester dihydroxybenzoyl moiety (ring B), which is located in the proximity of Phe31. To accommodate this ring, the Leu22 side chain adopts a different orientation than in the original DHFR structure used in TMECG modeling (PDB ID: 1S3V).<sup>[23]</sup> The ester-bound gallate moiety (ring D) of TMECG is accommodated in an amphiphilic region of DHFR involving residues Glu35, Asn64, and Leu67.

As expected, TMECG adopts a different orientation in the active site of human DHFR (Figure 3B). Although the ring A phenolic group maintained a hydrogen bond interaction with the side chain of Glu30 (O–O distance 2.91 Å), rings B and D occupied different positions within the enzyme active site. Several observations suggest that the position of TMECG in the human DHFR active site may be more favorable than that of TMECG, which could explain the higher DHFR inhibitory potency of TMECG. Ring B adopts a more favorable position by

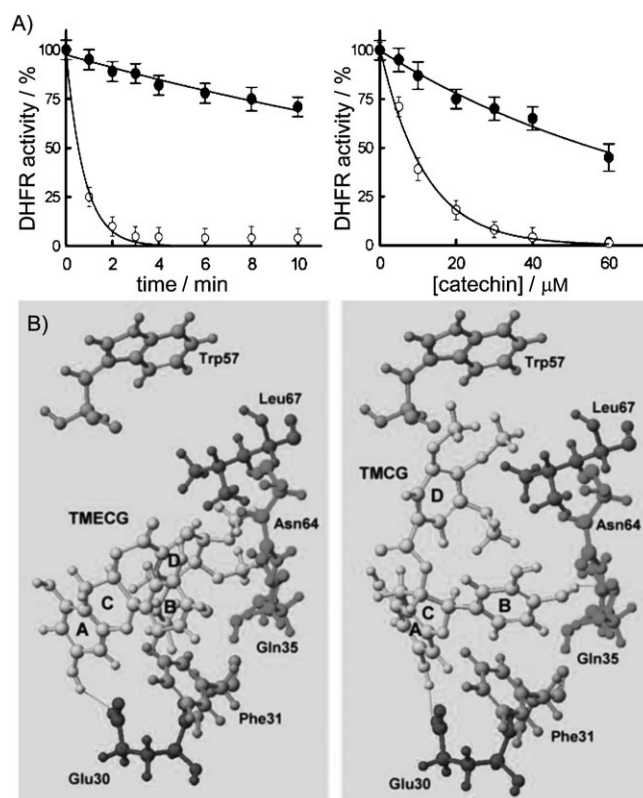


**Figure 3.** Kinetics and molecular modeling of human DHFR inhibition by TMECG and TMECG. A) Effect of pre-incubation times and catechin concentrations on the inhibition of DHFR by TMECG (●) and TMECG (○). To assess the effect of pre-incubation time, experiments were performed in the presence of 40 μM TMECG or TMECG. To assess the effect of catechin concentration, DHFR was pre-incubated with TMECG or TMECG for 10 min. B) View of TMECG and TMECG modeled into the folate binding site of human DHFR. The folate active site of human DHFR is a hydrophobic pocket ~15 Å wide, in which the only polar side chain is the Glu30 carbonyl group.<sup>[39]</sup> Other residues composing this active site are Ile7, Leu22, Gln35, Trp24, Asn64, Val115, and Thr136. Only residues in the active site or in its proximity that interact with TMECG and TMECG are highlighted. Phe34, which is located near TMECG ring D, is not labeled for the purpose of clarity. Specific hydrogen bonds between TMECG and Glu30 and between TMECG and Glu30 and Asn64 are indicated (-----).

moving away from Phe31, allowing Leu22 to adopt its usual position within the human DHFR structure. Ring B of TMECG is also located within hydrogen bonding distance of Gln35 (O–O distance 2.96 Å) (Figure 3B). This residue can form a hydrogen bond with the  $\alpha$ -carboxylate group of the glutamyl moiety of MTX in mouse and human DHFRs,<sup>[24,25]</sup> and its mutation can yield catalytically active MTX-resistant mutants.<sup>[26]</sup> Therefore, the presence of an additional hydrogen bond between Gln35 and the ring B hydroxy group of TMECG could stabilize the enzyme–inhibitor complex. Finally, the trimethoxylated moiety of TMECG (ring D) can interact with the protein through Trp57 and Phe34 (Figure 3B). A similar orientation was discovered in several quinazolinone analogues,<sup>[27]</sup> where binding to DHFR was stabilized through hydrogen bonds with Thr56, Trp57, and Phe58. Although our molecular modeling studies did not predict additional hydrogen bonds at these positions, the proximity of the methoxy groups of ring D to Trp57 and

Phe34 indicated that these hydrophobic interactions would favor binding of TMCG.

### Tyrosinase activation of TMECG and TMCG in melanoma cells

Despite the observed differences between the actions of these two epimers against non-melanoma cells, both compounds exhibited higher activities against melanoma cells (Figure 1). As has been described for TMECG,<sup>[10–12,28]</sup> TMCG downregulated DHFR in SK-MEL-28 melanoma cells (as demonstrated by mRNA and protein expression) and modulated Bax/Bcl-2 expression to a ratio favoring apoptosis (Figure 4). We have recently reported that the elevated activity of TMECG against melanoma was due to its cellular activation by tyrosinase.<sup>[11]</sup> Kinetic and spectroscopic data indicated that tyrosinase oxidized TMECG to its corresponding *o*-quinone, which quickly evolved through a series of chemical reactions to a quinone methide (QM) with high stability over a wide pH range.<sup>[11]</sup> The QM was found to be a potent irreversible inhibitor of human DHFR, and this highly stable product may be responsible for the high activity of TMECG against melanoma cells.<sup>[11]</sup> This hypothesis was also confirmed by experiments designed to show the activity of natural catechin EGCG in melanoma cells. EGCG was moderately active toward SK-MEL-28 melanoma cells (Figure 1) and was unable to induce apoptosis (Figure 4A). Cells treated with EGCG showed an evident increase in their melanin content, which may be related to the instability of the quinonic products derived from oxidation of EGCG by tyrosinase at the unprotected ring D hydroxy groups. EGCG cannot produce a stable QM after oxidation by tyrosinase, and it appears that these oxidation products can incorporate directly into melamins.

Oxidation of TMCG and TMECG by tyrosinase is predicted to generate the same final product, as proton-catalyzed hydrolysis of ring C would generate a freely rotating carbon (C3) which should prevent epimeric differences in the QM product (Scheme 2). To confirm that TMECG and TMCG generate the same quinonic product after tyrosinase oxidation, both substrates were oxidized *in vitro* using mushroom tyrosinase as a catalyst. The final products of corresponding oxidations were analyzed and compared using several spectroscopic techniques. Tyrosinase oxidized TMECG and TMCG to stable final products, which varied in color from yellow to orange in a pH-dependent manner. The products had similar spectroscopic properties, with  $\lambda_{\max}$  at 275/412 nm at acidic pH and 275/470 nm at higher pH values ( $pK_s=6.9$ ) (Figure 5A). UV/Vis spectroscopy data indicated that, as represented in Scheme 2, both TMECG and TMCG generated the same QM product following tyrosinase oxidation. Mass spectroscopy confirmed these results, and the spectra of both final oxidation products exhibited the same molecular ion peak. High-performance liquid chromatography–mass spectrometry (HPLC–MS) revealed that the molecular weights of the compounds were 498.7 and 498.8 for TMECG and TMCG, respectively, corresponding to the calculated mass of the QM product depicted in Scheme 2 (Figure 5B). Both molecules were analyzed by

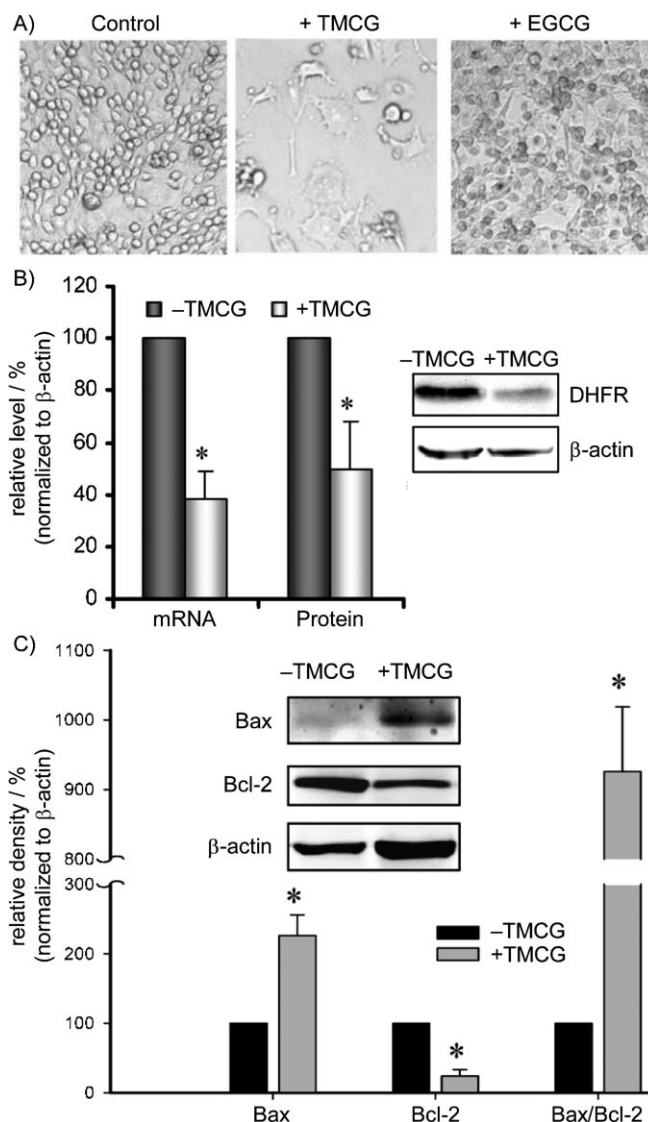
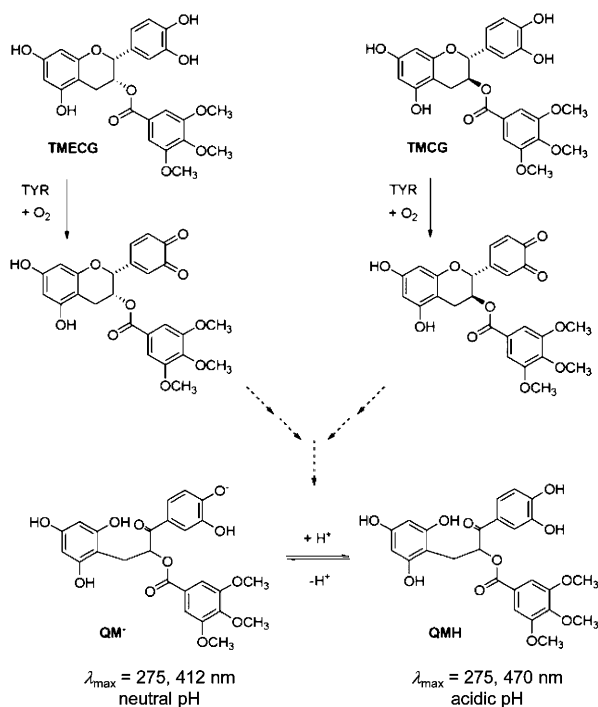


**Figure 4.** Effect of TMCG on SK-MEL-28 melanoma cells. A) Morphological aspects of untreated SK-MEL-28 cells (control) relative to those subjected to five days of treatment with TMCG and EGCG (both at 20  $\mu\text{M}$ ). B) Effect of TMCG on DHFR mRNA and protein expression in SK-MEL-28 cells. Data were obtained by real-time PCR and western blot analysis of samples of SK-MEL-28 cells treated with 10  $\mu\text{M}$  TMCG for three days (mRNA) and five days (protein). C) TMCG treatment resulted in a decrease in Bcl-2 and an increase in Bax, resulting in a significant increase in the Bax/Bcl-2 ratio that favors apoptosis. Data were obtained by western blot analysis from samples of SK-MEL-28 cells treated with 50  $\mu\text{M}$  TMCG for five days. In all cases, protein and/or mRNA levels were normalized with respect to  $\beta$ -actin and to their respective controls (100%). In panels B) and C),  $*p < 0.05$  relative to their respective controls (-TMCG).

MS–MS and produced the same daughter ion peaks at  $m/z$  363 and  $m/z$  287, corresponding to loss of the dihydroxybenzoyl or trimethoxybenzoyl moiety, respectively.

TMCG was slightly more active than TMECG at inhibiting cell growth ( $IC_{50}$  at six days:  $1.5 \pm 0.2$  and  $2.9 \pm 0.3$   $\mu\text{M}$  for TMCG and TMECG, respectively) (Figure 1) and inducing apoptosis (Figure 6A) in melanoma cells. Because bioavailability is not affected by epimerization,<sup>[29]</sup> we analyzed the oxidation of these compounds by tyrosinase to elucidate the cause of their different degrees of activity against melanoma. The catalytic effi-



**Scheme 2.** Reaction sequences indicating the oxidation of TMECG and TMCG by tyrosinase (TYR) and the formation of quinone methide (QM) species.

ciency of tyrosinase toward TMCG ( $6.9 \text{ min}^{-1} \text{ mM}^{-1}$ ) was four-fold higher than for TMECG ( $1.7 \text{ min}^{-1} \text{ mM}^{-1}$ ), indicating that tyrosinase activation of TMCG may be favored over TMECG in melanoma cells. To confirm these observations, the formation

of QM inside melanoma cells was analyzed using HPLC–MS–MS of cell extracts after treatment with TMCG or TMECG. The concentration of accumulated QM in SK-MEL-28 cells was significantly higher (3.6-fold) in cells treated with  $10 \mu\text{M}$  TMCG for 24 h than the concentration of accumulated QM in cells treated with TMECG under the same conditions (Figure 6B). A control experiment in which MDA-MD-231 breast cancer cells were treated with TMCG or TMECG under the same conditions demonstrated that QM was formed only in cells containing the melanocytic enzyme tyrosinase.

## Conclusions

Some natural catechins, such as ECG or EGCG, inhibit cancer cell proliferation.<sup>[30–33]</sup> To avoid therapeutic problems associated with poor stability and low cellular uptake of these compounds, derivative compounds TMECG and TMCG were synthesized. TMCG may be more appropriate and effective than TMECG for the treatment of non-melanoma epithelial cancer cells. The synthesis of TMCG was simpler and more economical than the synthesis of TMECG, and its effectiveness in inhibiting cell growth and inducing apoptosis in human breast, colon, and lung cell lines was significantly higher than that observed for TMECG. To understand the differences in the actions of these epimeric compounds, we tested various possibilities and observed large differences in their abilities to inhibit human DHFR. Although both compounds exhibited characteristics of slow-binding inhibitors, TMCG was sixfold more potent than TMECG, as deduced from their overall inhibition constants (Table 1). A crucial factor in the inhibition process is the disso-

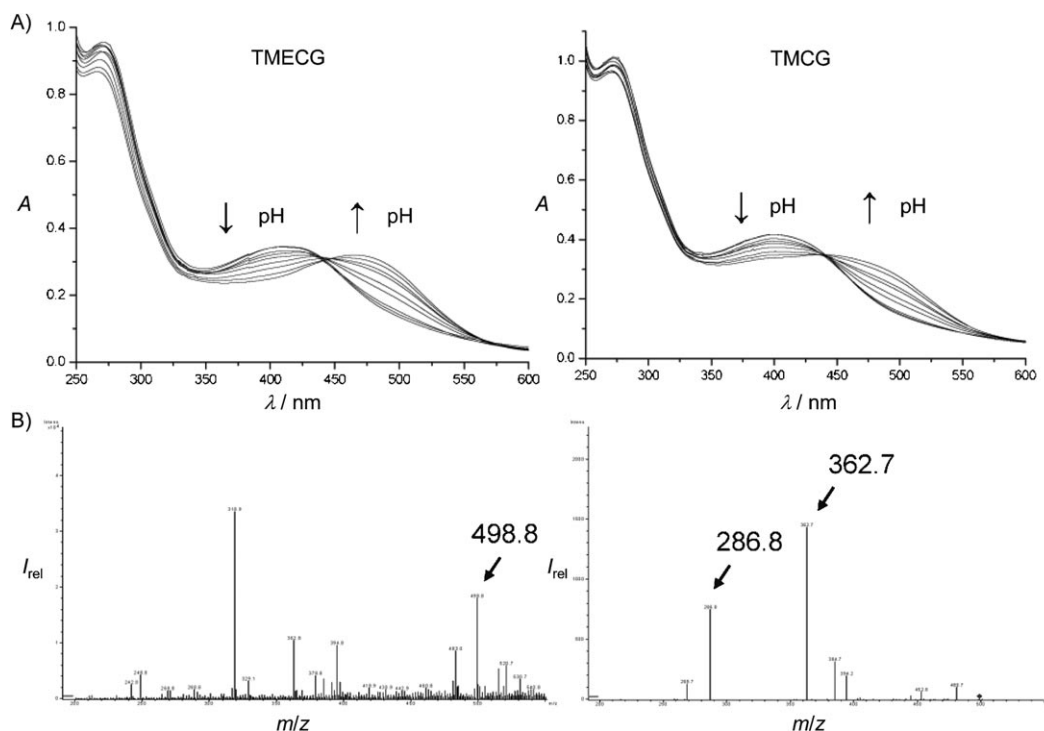


**Figure 5.** Analysis and comparison of the final products generated from the oxidation of TMECG and TMCG by mushroom tyrosinase (TMECG-QM and TMCG-QM, respectively). A) UV/Vis absorption spectra of TMECG-QM and TMCG-QM at various pH values. B) Mass spectra of TMECG-QM and MS–MS daughter ion mass spectra of the molecular ion peak at  $m/z$  499. TMECG-QM generated the same MS and MS–MS spectroscopic results.

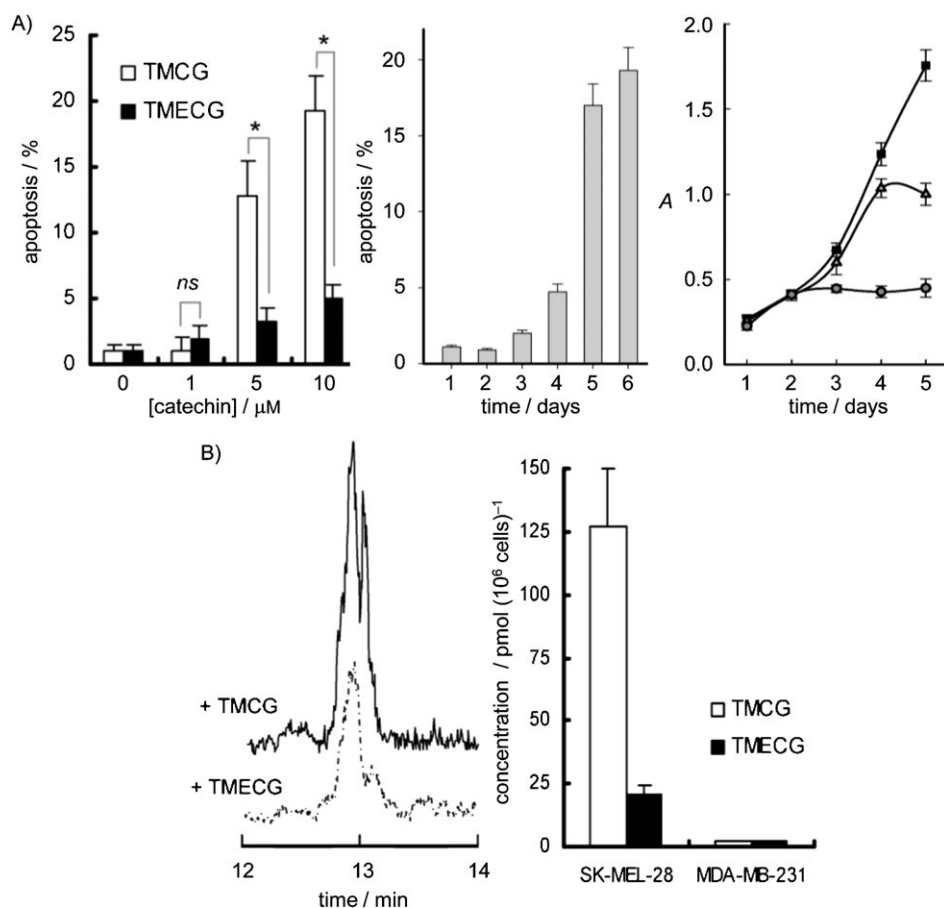


**Figure 6.** Differences between the actions of TMECG and TMCG in melanoma cells. A) Induction of apoptosis by TMECG and TMCG in SK-MEL-28 melanoma cells after six days of treatment. The differences in apoptosis induced by the two compounds were statistically significant for treatments with 5 and 10  $\mu\text{M}$  drug ( $*p < 0.05$ ); *ns*: not significant (left panel). Time-dependent apoptosis induction of TMCG (10  $\mu\text{M}$ ) on SK-MEL-28 (middle panel). Effect of 10  $\mu\text{M}$  (▲) and 20  $\mu\text{M}$  (●) TMCG on SK-MEL-28 growth determined by the MTT assay and compared with an untreated control (■) (right panel). B) Accumulation of QM species in SK-MEL-28 and MDA-MB-231 cells after 24 h treatments with TMCG and TMECG (both at 10  $\mu\text{M}$ ). The left panel represents the HPLC-MS chromatograms.

ciation constant of the E\*1 complex, which was found to be irreversible to a greater extent when using TMCG. A possible explanation for the irreversibility of this slowly dissociating enzyme complex is provided by molecular modeling.

The differential action of TMCG and TMECG against melanoma cells cannot be explained by the differences in their abilities to inhibit DHFR. Both compounds are prodrugs that are selectively activated in melanoma by the melanogenic enzyme tyrosinase, which transforms TMCG and TMECG to the same QM product. Therefore, the slight but statistically significant differences in the action of these drugs against melanoma are due to the different specific activities of tyrosinase toward TMCG and TMECG. In terms of activity, TMCG was a more effective drug for the treatment of melanoma; however, TMECG would be a more appropriate prodrug in regard to tumor selectivity. Antifolate compounds are designed to inhibit DHFR and act specifically during DNA and RNA synthesis, making them more toxic to rapidly dividing cells. This characteristic also results in antifolates that are unspecific for tumor cells and produces adverse side effects in rapidly dividing healthy

cells. Antifolate prodrugs designed to be specifically activated in tumor cells represent an attractive alternative that could prevent these undesirable side effects.<sup>[34]</sup> From this point of view, TMECG would be considered a better prodrug against melanoma. The decreased antifolate character of the TMECG prodrug relative to TMCG (Table 1) would favor specific activity against melanoma cells and prevent unspecific side effects in rapidly dividing healthy cells.

## Experimental Section

### Materials

Highly purified tea EGCG (>95%) was purchased from Sigma Chemical Co. (Madrid, Spain). Human DHFR was expressed in *Bombyx mori* chrysalides and purified by MTX-affinity chromatography.<sup>[35]</sup> Enzyme concentration was determined by MTX titration of enzyme fluorescence.<sup>[36]</sup> NADPH and dihydrofolic acid (DHF) were obtained from Sigma. Mushroom tyrosinase, Bcl-2,  $\beta$ -actin, and DHFR antibodies were purchased from Sigma, and the antibody against Bax was from Santa Cruz Biotechnology (Santa Cruz, CA, USA).

### Synthesis

All reactions were carried out using solvents that were dried by routine procedures.  $^1\text{H}$  and  $^{13}\text{C}$  NMR spectra were recorded on Bruker Avance 300 MHz and Bruker Avance 400 MHz instruments. The following abbreviations are used to represent the multiplicity of the signals: s (singlet), d (doublet), dd (double doublet), m (multiplet), and q (quaternary carbon atom). Chemical shifts are given with reference to the signals of  $(\text{CH}_3)_4\text{Si}$  in  $^1\text{H}$  and  $^{13}\text{C}$  NMR spectra. Electrospray (ES) mass spectra were recorded on Agilent 6220 TOF and Agilent VL spectrometers. Elemental analyses were performed on a Carlo Erba EA-1108 elemental analyzer. Melting points were determined on a Kofler hot-plate melting point apparatus and are uncorrected. Compounds 1, 2, and 3 were obtained using experimental procedures described elsewhere,<sup>[14]</sup> and their spectral data correlate with previously reported data.<sup>[14,18]</sup> Compounds used in biological tests possess purity higher than 98% as determined by elemental analysis.

**5,7,3',4'-Tetra-O-benzyl-3-(3'',4'',5''-trimethoxybenzoyl)-(-)-catechin (7):** A solution of 4 (1.41 g, 6.14 mmol) in dry  $\text{CH}_2\text{Cl}_2$  (5 mL) was added dropwise under nitrogen atmosphere to a solution containing 1 (2 g, 3.07 mmol) and 4-dimethylaminopyridine (DMAP; 0.94 g, 7.68 mmol) in the same solvent (30 mL). The reaction mix-

ture was stirred at room temperature for 18 h. A solution of saturated sodium bicarbonate (40 mL) was added, and the mixture was extracted twice with EtOAc (2 × 30 mL). The organic layers were then extracted twice with H<sub>2</sub>O (2 × 30 mL) and dried with anhydrous magnesium sulfate, and the solvent was removed under vacuum. The resulting yellow oil was subjected to silica gel column chromatography using *n*-hexane/EtOAc/CH<sub>2</sub>Cl<sub>2</sub> (6:6:2) as a solvent. The solvent was removed under reduced pressure, and the solid was recrystallized from Et<sub>2</sub>O/*n*-hexane to obtain a white solid (yield = 98%). *R*<sub>f</sub> = 0.76 (*n*-hex/EtOAc/CH<sub>2</sub>Cl<sub>2</sub> = 6:6:2); mp: 123–124 °C; <sup>1</sup>H NMR (CDCl<sub>3</sub>, 300 MHz): δ = 7.31–7.12 (m, 20H, Ph), 7.02 (s, 2H, H2'' and H6''), 6.97 (d, 1H, <sup>4</sup>J = 1.8 Hz, H2'), 6.88 (dd, 1H, <sup>3</sup>J = 8.2 Hz, <sup>4</sup>J = 1.8 Hz, H6'), 6.80 (d, 1H, <sup>3</sup>J = 8.2 Hz, H5'), 6.21 (d, 1H, <sup>4</sup>J = 2.4 Hz, H6), 6.19 (d, 1H, <sup>4</sup>J = 2.4 Hz, H8), 5.38 (m, 1H, H3), 5.04 (s, 2H, CH<sub>2</sub>O), 5.00 (m, 1H, H2), 4.98 (s, 2H, CH<sub>2</sub>O), 4.93 (s, 4H, 2 × CH<sub>2</sub>O), 3.79 (s, 3H, OCH<sub>3</sub>), 3.72 (s, 6H, OCH<sub>3</sub>), 3.05 (m, 1H, Hgem, H4), 2.76 ppm (m, 1H, Hgem, H4); <sup>13</sup>C NMR (CDCl<sub>3</sub>, 75 MHz): δ = 165.1 (q, -COO), 158.8 (q, Ar-O), 157.6 (q, Ar-O), 154.9 (q, Ar-O), 152.7 (2 × q, Ar-O), 149.0 (q, Ar-O), 148.9 (q, Ar-O), 142.2 (q, Ar-O), 136.9 (q, PhCH<sub>2</sub>), 136.8 (q, PhCH<sub>2</sub>), 136.7 (2 × q, PhCH<sub>2</sub>), 130.9 (q, C1'), 128.5 (CH, PhCH<sub>2</sub>), 128.4 (CH, PhCH<sub>2</sub>), 128.3 (2 × CH, PhCH<sub>2</sub>), 127.9 (CH, PhCH<sub>2</sub>), 127.8 (CH, PhCH<sub>2</sub>), 127.7 (2 × CH, PhCH<sub>2</sub>), 127.4 (CH, PhCH<sub>2</sub>), 127.3 (CH, PhCH<sub>2</sub>), 127.1 (2 × CH, PhCH<sub>2</sub>), 124.8 (q, C1''), 120.0 (CH, C6'), 114.7 (CH, C5'), 113.4 (CH, C2'), 106.7 (CH, C2'' and C6''), 101.4 (q, C4a), 94.3 (CH, C6), 93.7 (CH, C8), 78.4 (CH, C2), 71.3 (CH<sub>2</sub>, CH<sub>2</sub>Ph), 71.1 (CH<sub>2</sub>, CH<sub>2</sub>Ph), 70.1 (CH, C3), 70.0 (CH<sub>2</sub>, CH<sub>2</sub>Ph), 69.8 (CH<sub>2</sub>, CH<sub>2</sub>Ph), 60.8 (CH<sub>3</sub>, OCH<sub>3</sub>), 56.1 (CH<sub>3</sub>, OCH<sub>3</sub>), 24.6 ppm (CH<sub>2</sub>, C4); ESMS *m/z* (%) 845.3 ([M<sup>+</sup> + 1], 100); Anal. calcd for C<sub>33</sub>H<sub>48</sub>O<sub>10</sub> (844.3): C 75.34, H 5.73, found: C 75.21, H 5.84.

**3-O-(3,4,5-Trimethoxybenzoyl)-(–)-catechin (8):** Under normal pressure, a solution of **7** (1.5 g, 1.77 mmol) and 10% Pd/C (0.05 g Pd, 0.47 mmol) in THF/MeOH (3:1) (40 mL) was treated with H<sub>2</sub>. The solution was stirred for 14 h at room temperature and then filtered through a Celite pad, which was washed afterward with CH<sub>2</sub>Cl<sub>2</sub>/MeOH (9:1) (200 mL). The solvent was removed under vacuum, and the resulting solid was recrystallized from Et<sub>2</sub>O (90% yield). *R*<sub>f</sub> = 0.18 (*n*-hexane/EtOAc/CH<sub>2</sub>Cl<sub>2</sub> = 6:6:2); mp: 109–110 °C; <sup>1</sup>H NMR ([D<sub>6</sub>]acetone, 400 MHz): δ = 8.42 (bs, 1H, OH), 8.19 (bs, 1H, OH), 7.99 (bs, 1H, OH), 7.98 (bs, 1H, OH), 7.13 (s, 2H, H2'' and H6''), 7.00 (d, 1H, <sup>4</sup>J = 1.8 Hz, H2'), 6.87 (dd, 1H, <sup>3</sup>J = 8.1 Hz, <sup>4</sup>J = 1.8 Hz, H6'), 6.81 (d, 1H, <sup>3</sup>J = 8.1 Hz, H5'), 6.08 (d, 1H, <sup>4</sup>J = 2.4 Hz, H6), 5.97 (d, 1H, <sup>4</sup>J = 2.4 Hz, H8), 5.28 (m, 1H, H3), 5.05 (m, 1H, H2), 3.81 (s, 6H, OCH<sub>3</sub>), 3.75 (s, 3H, OCH<sub>3</sub>), 3.14 (m, 1H, Hgem, H4), 2.75 ppm (m, 1H, Hgem, H4); <sup>13</sup>C NMR ([D<sub>6</sub>]acetone, 100 MHz): δ = 165.6 (q, -COO), 158.0 (q, Ar-O), 157.2 (q, Ar-O), 156.5 (q, Ar-O), 153.9 (q, Ar-O), 145.8 (q, Ar-O), 145.7 (q, Ar-O), 143.2 (q, Ar-O), 131.0 (q, C1'), 126.0 (q, C1''), 119.5 (CH, C6'), 115.8 (CH, C5'), 114.7 (CH, C2'), 107.6 (CH, C2'' and C6''), 99.3 (q, C4a), 96.4 (CH, C6), 95.4 (CH, C8), 79.3 (CH, C2), 71.7 (CH, C3), 60.5 (CH<sub>3</sub>, CH<sub>3</sub>O), 56.4 (CH<sub>3</sub>, CH<sub>3</sub>O), 25.8 ppm (CH<sub>2</sub>, C4); ESMS *m/z* (%) 483.6 ([M<sup>+</sup> – 1], 100); Anal. calcd for C<sub>25</sub>H<sub>24</sub>O<sub>10</sub> (484.1): C 61.98, H 4.99, found: C 61.96, H 5.11.

<sup>1</sup>H and <sup>13</sup>C NMR, HMQC, and mass spectra for compounds **7** and **8** are provided in the Supporting Information.

## Biology

**Cell cultures:** Human cancer cell lines (SK-MEL-28, MDA-MB-231, N417, and Caco-2) were obtained from the American Type Culture Collection (ATCC) and were maintained in appropriate culture media supplemented with 10% fetal calf serum and antibiotics under standard tissue culture conditions. Cell viability was evaluated by a colorimetric assay for mitochondrial function using the 3-

(4,5-dimethylthiazol-2-yl)-2,5-diphenyltetrazolium bromide (MTT; Sigma) cell proliferation assay.<sup>[37]</sup> For this assay, cells were plated in a 96-well plate at a density of 1000–2000 cells per well. Compounds were added once at the beginning of each experiments.

**Apoptosis assays:** Apoptosis induction was assessed by analyzing cytoplasmic histone-associated DNA fragmentation with a kit from Roche Diagnostics (Barcelona, Spain). Apoptosis was determined as the specific enrichment of mono- and oligonucleosomes released into the cytoplasm and was calculated by dividing the absorbance of treated samples by the absorbance of untreated controls. The Annexin-V-FLUOS Staining Kit from Roche Diagnostics was used to detect cell apoptosis. Annexin-V staining was performed according to the manufacturer's protocols. After washing with PBS, cells were resuspended in 100 μL of Annexin-V-FLUOS labeling solution (containing PI and Annexin-V-fluorescein) and incubated for 15 min at room temperature in the dark. Cells were analyzed by flow cytometry in a Beckman Coulter Epics XL flow cytometer.

**Antioxidant activity:** The Trolox equivalent antioxidant capacity (TEAC) for each catechin was determined as described elsewhere.<sup>[10]</sup>

**NADPH oxidation by catechins:** The pro-oxidant activity of catechins was determined by their NADPH oxidation capacity.<sup>[10]</sup> The rate of NADPH (0.1 mM) oxidation at 37 °C was calculated in the presence of 50 μM catechins in sodium-phosphate buffer (pH 7.4) by following the decrease in absorbance of NADPH at 340 nm in a PerkinElmer Lambda-35 spectrophotometer.

**Inhibition of purified 20S proteasome activity:** The chymotrypsin-like activity of the 20S proteasome was measured by incubating 30 ng of purified rabbit 20S proteasome (Sigma) with 40 μM of the fluorescent peptide substrate Suc-Leu-Leu-Val-Tyr-AMC with and without synthetic catechins.

**DHFR activity assays:** The activity of DHFR in the absence or presence of catechins was determined at 25 °C by following the decrease in the absorbance of NADPH and DHF at 340 nm as described elsewhere.<sup>[5]</sup> Experiments to determine the recovery of enzyme activity after inhibition by pre-incubation with catechins were performed as follows. DHFR (165 nM) was pre-incubated for 10 min at 25 °C in the buffer mixture containing catechins at various concentrations. Aliquots (20 μL) of the incubation mixture were then diluted 50-fold into a reaction mixture containing the buffer mixture, NADPH (100 μM), and DHF (20 μM) to give a final enzyme concentration of 3.3 nM. Recovery of enzyme activity was followed by continuous monitoring at 340 nm.

**Fluorescence studies:** Dissociation constants for the binding of TMECG and TMCG to free human DHFR were determined by fluorescence titration in an automatic scanning FluoroMax-3 spectrofluorimeter (Jobin Yvon, Horiba, Edison, NJ, USA) with 1.0 cm light path cells and a 150 W Mercury–Xenon light source. Formation of a binary complex between the enzyme and the ligand was followed by measuring the quenching of tryptophan fluorescence of the enzyme upon addition of microliter volumes of a concentrated stock solution of ligand. Fluorescence emission spectra were recorded when human DHFR fluorescence was excited at 290 nm, and titrations were performed as described elsewhere.<sup>[5]</sup>

**Tyrosinase assays:** Catechin oxidation, catalyzed by mushroom tyrosinase, was followed at 440 nm (isosbestic point) using a Perkin-Elmer Lambda-35 spectrophotometer (Waltham, MA, USA). Experiments were performed in acetate buffer (pH 5.0).

**Real-time PCR:** Real-time PCR analysis was carried out as described elsewhere,<sup>[10]</sup> using the following primers for the amplification of human genes: *dhfr* (forward: 5'-ATG CCT TAA AAC TTA CTG AAC AAC CA-3'; reverse: 5'-TGG GTG ATT CAT GGC TTC CT-3'); *β-actin* (forward: 5'-AGA AAA TCT GGC ACC ACA CC-3'; reverse: 5'-GGG GTG TTG AAG GTC TCA AA-3').

**Western blotting:** Cells were lysed by sonication in PBS pH 7.4 containing 1% NP-40, 1% Triton X-100, 0.5% sodium deoxycholate, 0.1% SDS, and protease inhibitor cocktails. After centrifugation (15 000 g, 20 min), soluble proteins were separated by SDS-PAGE, transferred to nitrocellulose membranes, and analyzed by immunoblotting (ECL Plus, GE Healthcare).

### In silico molecular modeling

Molecular modeling was carried out using the CAChe software package v. 7.5 (Fujitsu, Krakow, Poland). In searching for available ligand-bound human DHFR structures in the PDB,<sup>[38]</sup> we identified a 1.8 Å structure (PDB ID: 1S3V)<sup>[27]</sup> that was the best available structural match for TMECG and TMCG. Hydrogen atoms were added to the DHFR molecules prior to docking procedures. TMECG and TMCG were built and energy minimized on CAChe. The molecular geometries of both compounds were optimized using MM3 molecular mechanics methods until the root mean square (RMS) gradient value was smaller than 0.1 kcal mol<sup>-1</sup>. The fastest and easiest method for docking a ligand into an active site is to superimpose the ligand on to a bound ligand already in the active site and then delete the bound ligand. Then, using the position of (R)-6-[(methyl-(3,4,5-trimethoxyphenyl)amino)methyl]-5,6,7,8-tetrahydroquinazoline-2,4-diamine as a guide, compounds were docked into this protein structure, and the energy of the inhibitor-protein composite was then minimized using MM3.

### UV/Vis spectroscopy

UV/Vis absorption spectra of TMECG-QM and TMCG-QM at different pHs were recorded on a UV/Vis PerkinElmer Lambda-35 spectrophotometer with a spectral bandwidth of 1 nm at a scan speed of 960 nm min<sup>-1</sup>. Experiments were performed in various buffers over pH range 5.0–9.0, with the pH of the reaction measured before and after the experiment.

### HPLC-MS

QM was analyzed on a HPLC-MS system consisting of an Agilent 1100 Series HPLC (Agilent Technologies) connected to an Agilent Ion Trap XCT Plus mass spectrometer (Agilent Technologies) using an electrospray (ESI) interface. To detect QM in cell extracts, cells were collected at the end of each incubation period, washed three times with PBS, and lysed by addition of a buffer containing 2 mM EDTA, 2 mM EGTA, 20 mM imidazole-HCl, and 50 mM ascorbic acid (pH 7). Ascorbic acid was included to avoid oxidation of catechins during the extraction process. After one hour of incubation at 4 °C, the lysates were sonicated and centrifuged. The supernatants were deproteinized by the addition of acetonitrile, and the solution was centrifuged to recover the supernatants, which were filtered on Microcon centrifugal filter devices with a mass cutoff of 10 000 units (Millipore). Filtrates were lyophilized and resuspended in 50 μL acetonitrile. The resulting suspensions were centrifuged, and the supernatants were analyzed by HPLC-MS-MS. Analysis was carried out using the same HPLC-MS system.

### Statistical analysis

In all experiments, the mean ± standard deviation (SD) values for three to five determinations in triplicate were calculated. Statistically significant differences were evaluated using the Student's *t*-test. Differences were considered statistically significant at *p* < 0.05.

### Acknowledgements

This work was supported in part by grants from the Ministerio de Ciencia e Innovación (MICINN), Spain (project SAF2009-12043-C02-01) and the Fundación Séneca, Región de Murcia (FS-RM), Spain (project 08595/PI/08) to J.N.R.-L. and J.C.-H., and from the MICINN (project CTQ2008-01402) and the FS-RM (project 04509/GERM/06) to A.T. J.C.-H. is contracted by the Translational Cancer Research Group (Fundación para la Formación e Investigación Sanitarias (FFIS); Murcia, Spain). M.S.-A. has a fellowship from the MICINN. L.S.-d.-C. has a fellowship from the FS-RM. S.C. is contracted by the program "Torres Quevedo" from the MICINN, and M.F.M. is contracted by an agreement with the Fundación de la Asociación Española contra el Cáncer (FAECC).

**Keywords:** antifolate activity • epimers • melanoma • prodrugs • tea catechins

- [1] E. Navarro-Perán, J. Cabezas-Herrera, F. García-Cánovas, M. C. Durrant, R. N. F. Thorneley, J. N. Rodríguez-López, *Cancer Res.* **2005**, *65*, 2059–2064.
- [2] N. C. Alemdaroglu, S. Wolfram, J. P. Boissel, E. Closs, H. Spahn-Langguth, P. Langguth, *Planta Med.* **2007**, *73*, 27–32.
- [3] E. Navarro-Perán, J. Cabezas-Herrera, L. Sánchez del Campo, J. N. Rodríguez-López, *Int. J. Biochem. Cell Biol.* **2007**, *39*, 2215–2225.
- [4] M. D. Navarro-Martínez, F. García-Cánovas, J. N. Rodríguez-López, *J. Antimicrob. Chemother.* **2006**, *57*, 1083–1092.
- [5] E. Navarro-Perán, J. Cabezas-Herrera, A. N. P. Hiner, T. Sadunishvili, F. García-Cánovas, F. J. N. Rodríguez-López, *Biochemistry* **2005**, *44*, 7512–7525.
- [6] M. Spina, M. Cuccioloni, M. Mozzicafreddo, F. Montecchia, S. Pucciarelli, A. M. Eleuteri, E. Fioretti, M. Angeletti, *Proteins* **2008**, *72*, 240–251.
- [7] T. T. Kao, K. C. Wang, W. N. Chang, C. Y. Lin, B. H. Chen, H. L. Wu, G. Y. Shi, J. N. Tsai, T. F. Fu, *Drug Metab. Dispos.* **2008**, *36*, 508–516.
- [8] P. Hannewald, B. Maunit, J. F. Muller, *Anal. Bioanal. Chem.* **2008**, *392*, 1335–1344.
- [9] J. Hong, H. Lu, X. Meng, J. H. Ryu, Y. Hara, C. S. Yang, *Cancer Res.* **2002**, *62*, 7241–7246.
- [10] L. Sánchez-del-Campo, F. Otón, A. Tárraga, J. Cabezas-Herrera, S. Chazarra, J. N. Rodríguez-López, *J. Med. Chem.* **2008**, *51*, 2018–2026.
- [11] L. Sánchez-del-Campo, A. Tárraga, M. F. Montenegro, J. Cabezas-Herrera, J. N. Rodríguez-López, *Mol. Pharm.* **2009**, *6*, 883–894.
- [12] L. Sánchez-del-Campo, J. N. Rodríguez-López, *Int. J. Cancer* **2008**, *123*, 2446–2455.
- [13] M. Babich, H. L. Zuckerbraun, S. M. Weinerman, *Toxicol. Lett.* **2007**, *171*, 171–180.
- [14] W. Tückmantel, A. P. Kozikowski, J. J. Romanczyk, Jr., *J. Am. Chem. Soc.* **1999**, *121*, 12073–12081.
- [15] K. D. Park, S. G. Lee, S. U. Kim, S. H. Kim, W. S. Sun, S. J. Cho, D. H. Jeong, *Bioorg. Med. Chem. Lett.* **2004**, *14*, 5189–5192.
- [16] S. Azam, N. Hadi, N. U. Khan, S. M. Hadi, *Toxicol. In Vitro* **2004**, *18*, 555–561.
- [17] S. Nam, D. M. Smith, Q. P. Dou, *J. Biol. Chem.* **2001**, *276*, 13322–13330.
- [18] S. B. Wan, D. Chen, Q. P. Dou, T. H. Chan, *Bioorg. Med. Chem.* **2004**, *12*, 3521–3527.
- [19] K. Osanai, K. R. Landis-Piwowar, Q. P. Dou, T. H. Chan, *Bioorg. Med. Chem.* **2007**, *15*, 5076–5082.

- [20] K. R. Landis-Piwowar, S. B. Wan, R. A. Wiegand, D. J. Kuhn, T. H. Chan, Q. P. Dou, *J. Cell. Physiol.* **2007**, *213*, 252–260.
- [21] J. D. Lambert, C. S. Yang, *J. Nutr.* **2003**, *133*, 3262S–3267S.
- [22] C. Huo, S. B. Wan, W. H. Lam, L. Li, Z. Wang, K. R. Landis-Piwowar, D. Chen, Q. P. Dou, T. H. Chan, *Inflammopharmacology* **2008**, *16*, 248–252.
- [23] V. Cody, J. R. Luft, W. Pangborn, A. Gangjee, S. F. Queener, *Acta Crystallogr. Sect. D* **2004**, *60*, 646–655.
- [24] D. K. Stammers, J. N. Champness, C. R. Beddell, J. G. Dann, E. Eliopoulos, A. J. Geddes, D. Ogg, A. C. North, *FEBS Lett.* **1987**, *218*, 178–184.
- [25] V. Cody, J. R. Luft, W. Pangborn, *Acta Crystallogr. Sect. D* **2005**, *61*, 147–155.
- [26] J. P. Volpato, E. Fossati, J. N. Pelletier, *J. Mol. Biol.* **2007**, *373*, 599–611.
- [27] S. T. Al-Rashood, I. A. Aboldahab, M. N. Nagi, L. A. Abouzeid, A. A. M. Andel-Aziz, S. G. Andel-Hamide, K. M. Youssef, A. M. Al-Obaid, H. I. El-Subbagh, *Bioorg. Med. Chem.* **2006**, *14*, 8608–8621.
- [28] L. Sánchez-del-Campo, S. Chazarra, M. F. Montenegro, J. Cabezas-Herrera, J. N. Rodríguez-López, *J. Cell. Biochem.* **2010**, *110*, 1399–1409.
- [29] J. Z. Xu, S. Y. V. Yeung, Q. Chang, Y. Huang, Z.-Y. Chen, *Br. J. Nutr.* **2004**, *91*, 873–881.
- [30] Y. D. Jung, L. M. Ellis, *Int. J. Exp. Pathol.* **2001**, *82*, 309–316.
- [31] Y. D. Hsuuw, W. H. Chan, *Ann. N. Y. Acad. Sci.* **2007**, *1095*, 428–440.
- [32] G. Y. Yang, J. Liao, K. Kim, E. J. Yurkow, C. S. Yang, *Carcinogenesis* **1998**, *19*, 611–616.
- [33] M. Nihal, N. Ahmad, H. Mukhtar, G. S. Wood, *Int. J. Cancer* **2005**, *114*, 513–521.
- [34] M. Rooseboom, J. N. M. Commandeur, N. P. E. Vermeulen, *Pharmacol. Rev.* **2004**, *56*, 53–102.
- [35] S. Chazarra, S. Aznar-Cervantes, L. Sánchez-del-Campo, J. Cabezas-Herrera, W. Xiaofeng, J. L. Cenis, J. N. Rodríguez-López, *Appl. Biochem. Biotechnol.* **2010**, *162*, 1834–1846.
- [36] S. L. Smith, P. Patrick, D. Stone, A. W. Phillips, J. J. Burchall, *J. Biol. Chem.* **1979**, *254*, 11 475–11 484.
- [37] T. Mosmann, *J. Immunol. Methods* **1983**, *65*, 55–63.
- [38] H. M. Berman, J. Westbrook, Z. Feng, G. Gilliland, T. N. Bhat, H. Weissig, I. N. Shindyalov, P. E. Bourne, *Nucleic Acids Res.* **2000**, *28*, 235–242.
- [39] S. J. Benkovic, C. A. Fierke, A. M. Naylor, *Science* **1988**, *239*, 1105–1110.

---

Received: November 10, 2010

Revised: December 23, 2010

Published online on February 7, 2011